NANO LETTERS

2007
Vol. 7, No. 2
513−519

Nanoscale Engineering of a Cellular Interface with Semiconductor Nanoparticle Films for Photoelectric Stimulation of Neurons

Todd C. Pappas,[†] W. M. Shan Wickramanyake,[‡] Edward Jan,[‡] Massoud Motamedi,[†,§] Malcolm Brodwick,[§] and Nicholas A. Kotov*[,‡]

Center for Biomedical Engineering, University of Texas Medical Branch, Galveston, Texas 77555-0456, Department of Chemical Engineering, Department of Biomedical Engineering, and Department of Materials Science, 2300 Hayward Street, University of Michigan, Ann Arbor, Michigan 48109, and Department of Neuroscience and Cell Biology, University of Texas Medical Branch, Galveston, Texas 77555-0456

Received October 25, 2006; Revised Manuscript Received December 14, 2006

ABSTRACT

The remarkable optical and electrical properties of nanostructured materials are considered now as a source for a variety of biomaterials, biosensing, and cell interface applications. In this study, we report the first example of hybrid bionanodevice where absorption of light by thin films of quantum confined semiconductor nanoparticles of HgTe produced by the layer-by-layer assembly stimulate adherent neural cells via a sequence of photochemical and charge-transfer reactions. We also demonstrate an example of nanoscale engineering of the material driven by biological functionalities.

Introduction. Nanocolloids represent a tremendous resource for molecular engineering of novel biomaterials and implantable devices that could be effectively interfaced with the nervous system. The desirable features of nanoparticles are their unique quantum mechanical properties, exceptionally high surface area, and ease of chemical modification with biological ligands. Some of these features have already been exploited for other biomedical applications including imaging,[1] biosensing,[2,3] DNA analysis,[4] cancer treatment,[5−8] and drug delivery.[9−14] There is also a growing number of studies on biological responses to nanomaterials at the tissue and organ level[15−17] with carbon nanotube and some times nanowires being the most frequently used for interfacing with neurons.[18−24] We believe that nanomaterials also offer unique optical, electrical, and structural properties that may allow us to control stimulation of electrically excitable cells or groups of cells. These materials can be used to fabricate small, targetable, and remotely addressable (i.e., potentially wireless) electrodes, which could lead to the development of new therapeutic tools for neuronal injury, developmental dysfunction, and sensory deficits.

Many semiconductor and metal nanoparticles (NPs), also known as quantum dots, are photo- and electroactive. Unlike direct electrical excitation of neurons on bulk semiconductor devices, such as field-effect transistors,[25] the use of NPs takes advantage of quantum confinement effects. These properties can be exploited in layered NP structures that produce photocurrents. The photocurrent generated in these films can mediate extrinsic stimulation of cells, while quantum effects allow us to engineer films with the desired electrical and spectral responses. In this communication, we demonstrate for the first time (1) that these versatile photoactive nanomaterials can be used to stimulate neurons with light, (2) that the engineering of the interface between the NP films and neurons can play an essential role in the successful signal transduction from the inorganic film to live cells, and (3) potential methods for engineering of this interface.

Results and Discussion. As a model system, NP films (Figure 1A), were assembled by the layer-by-layer (LBL) technique[26−29] into tightly packed conductive composite films (Figure 1B).[30] Comparative images of the substrate and substrate + PDDA are given in Supporting Information (Figure S1). Photo/electroactive NP films were made from HgTe stabilized with thioglycolic acid. Poly(dimethyldial-

* Corresponding author. kotov@umich.edu.
[†] Center for Biomedical Engineering, University of Texas Medical Branch.
[‡] Department of Chemical Engineering, Department of Biomedical Engineering, and Department of Materials Science, University of Michigan.
[§] Department of Neuroscience and Cell Biology, University of Texas Medical Branch.

10.1021/nl062513v CCC: $37.00
Published on Web 12/29/2006

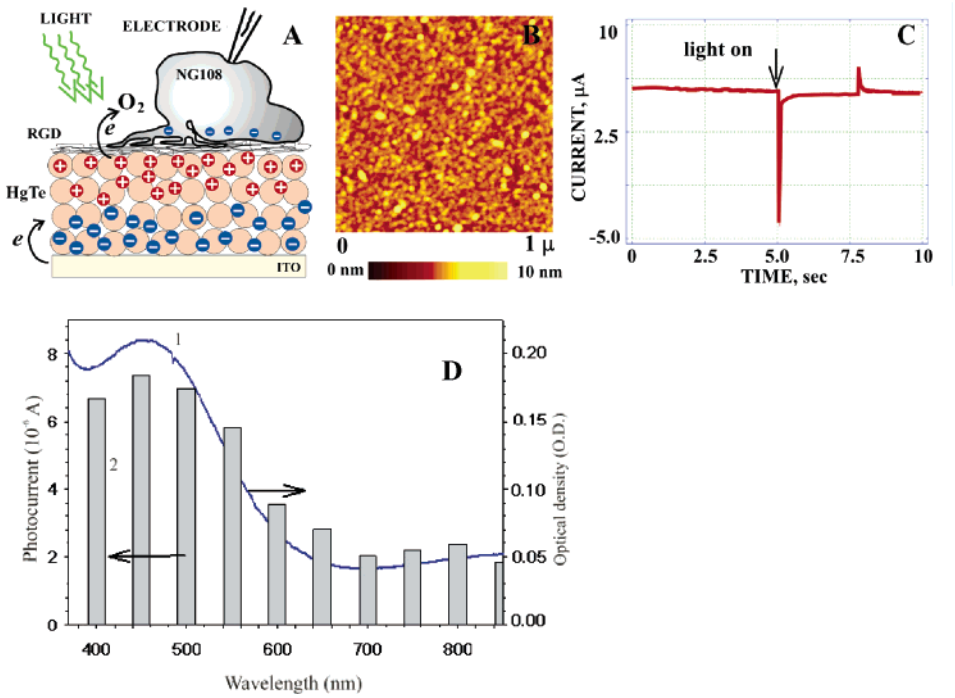

Figure 1. Photovoltaic properties of LBL films from HgTe. (A) Schematic of coupling between NP and the neuron. (B) Atomic force microscopy image of the $(HgTe/PDDA)_1$ on Si wafer. (C) Photocurrent response measured at 0.0 V bias for $(PDDA/HgTe)_{12}$ under monochromatic 550 nm illumination. Arrow indicates the onset of illumination. Electrodes: ITO glass with the NP film, working electrode; saturated Ag/AgCl, reference electrod; Ag wire, counter electrode, electroanalyzer/potentiostat Epsilon C50. $(PDDA/NP)_N$ films on ITO with and without neurons attached were immersed in HBS. The photovoltaic curves registered in a Teflon three-electrode photochemical cell were identical in shape and sign when registered with and without cells present on the surface. The ITO slide was illuminated through a glass window 3 cm in diameter. The light from an Oriel 1000W Xe was IR filtered through a water-filled quartz cuvette with optical path of 5 cm passed ether through an Oriel CornerStone monochromator and then impinged the surface of the NP film perpendicularly to the sample surface. In deaerated solutions the photocurrent was more than an order of magnitude smaller and anodic. Repeated stimulation of the NP thin film (up to 10 times) yielded responses that were similar in shape with some reduction of the current spike due to photocorrosion of HgTe. (D). Light absorption characteristics of HgTe NPs and LBL films. (1, solid line) UV−vis absorption spectrum on HgTe NP dispersion stabilized by thioglycerol used for fabrication of LBL films. (2, bars) Dependence of photogenerated voltage in $PDDA/HgTe)_{12}$PLP multilayer on the wavelength of incident light. The wavelengths for (2) were selected with corresponding diffraction filters. The intensity of illumination was measured with the laser power meter. The photocurrent was normalized for the illumination at 400 nm. Arrows in the graph point to the corresponding axes for each plot. The photocurrent data track light absorption spectrum of HgTe, which indicates that the charge carriers originate from excitons generated in the semiconductor by light quanta.

lylammonium chloride) (M_w = 450000−500000, PDDA) was employed as a positively charged macromolecular LBL partner of the HgTe nanocolloid. The LBL deposition cycle was initiated on indium tin oxide-coated (ITO) glass to provide an electron source. Layering was repeated N times, referred to as $(PDDA/NP)_N$, where N is the number of bilayers. The photocurrent was cathodic with transient characterized by the strong initial spike (Figure 1C). Electrons and holes were produced by excitons photogenerated in quantum-confined HgTe after absorption of UV−vis/IR quanta (Figure 1D) in a linear single photon process (Supporting Information Figure S2). It originates from the NP→O_2 photoinduced electron transfer: the energy of acceptor energy level in O_2 is −5.3 eV, while approximate position of the bottom of HgTe NP conduction band is −4.6 eV (both vs electron in vacuum). The registered current is produced by electrons injected from electrode in response to hole accumulation in the film when photogenerated electrons are removed by O_2^- (Figure 1A). The positive charge at the outer interface of the film is accumulated due to fairly slow electron transport through NP solids;[31] it exist there at least for the duration of the cathodic spike (Figure 1C).

The well-characterized neuroblastoma*glioma cell line NG108,[32] was chosen as a model neuronal cell for the nanobiodevice because it displays a distinct neuronal phenotype, including voltage-activated inward currents and action potentials (APs),[33] but is less sensitive to environmental conditions than primary neurons and could therefore be used to test media formulations for growth on NP thin films. NG108 cells (ATCC Manassas, VA) were routinely cultured in F12:DMEM (1:1) supplemented with 25 mM HEPES, 10% FBS, 0.1 mM hypoxanthine, 400 nM aminopterin, and 0.016 mM thymidine. We tested a number of reduced serum formulations for 24−72 h growth and differentiation on the NP thin films and found that NG108 showed complex neurites (Figure 2) and typical voltage-activated inward currents under whole-cell voltage clamp (see Supporting Information, Figure S3) when grown using F12/DMEM supplemented with 5% fetal bovine serum, 5 μM 3-isobutyl-1-methylxanthine, and 5 μM forskolin (both in DMSO, 0.01% (v/v)). We used LBL addition of polylysine/poly(acrylic acid)/polylysine (PLP) monolayers to improve biocompatibility and cell adhesion to $(PDDA/HgTe)_{12}$PLP multilayer stack, similar to our previous investigations.[34]

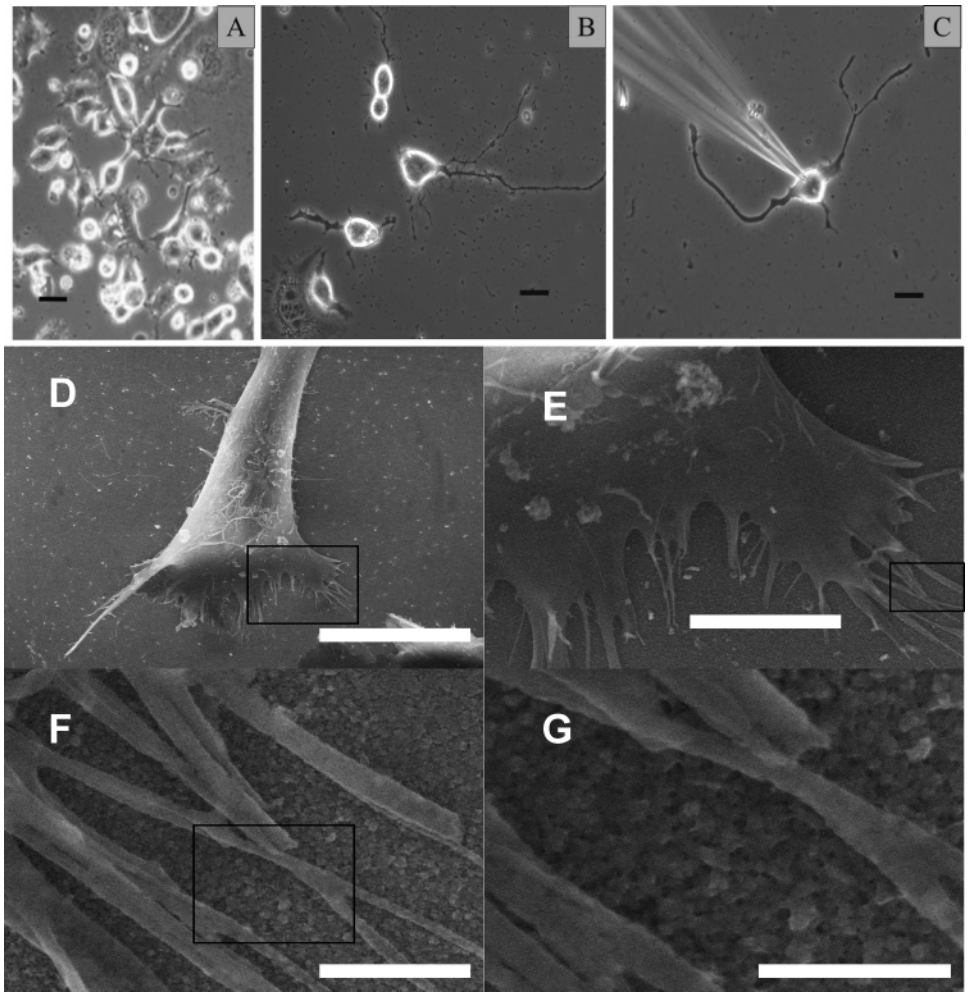

Figure 2. Microscopy images of NG108 on HgTe LBL films. (A) Optical phase contrast photomicrograph of NG108 grown on (PDDA/HgTe)$_{12}$PLP. (B, C) Microscopy images of one of the cells grown on (PDDA/HgTe)$_{12}$(PDDA/Clay)$_2$PLP. For images A and B and C, the scale bars are 20 and 10 μm, respectively. The cells were cultured on the films for 24 h. Neurons are well differentiated, which can be seen by long neuritis extending to different directions. In (C), the image of the patch clamp electrode used to measure the membrane currents and potential was captured as well. (D−G) Scanning electron microscopy images of one of the cells grown on LBL layers in the early stages of differentiation to avoid accumulation of large amount of biological material on the surface of NP layers. The black squares in D, E, and F show the areas, where the following image was taken. This image illustrates the surface porosity of the thin film where cell structures (neurites) and the film interact. Scale bars are 20, 5, 1.0, and 0.5 μm for D−G, respectively.

Further absorption of peptide predicted from fibronectin (CGGGRGDS) was used to increase both cell survival and attachment.[35,36] Parts D−G of Figure 2 show scanning electron micrographs of NG108 grown on a (PDDA/HgTe)$_{12}$PLP surface and illustrate the interaction of cell processes with the mesoporous surface of the NP thin film.

We tested the hybrid nanostructured device for its ability to phototransduce an electrical signal to neurons grown on the surface. NG108 cells were grown on the NP thin film previously sterilized with ethanol for 24−72 h. The NP thin film with cells was placed into a cover glass recording chamber, and media were changed to a HEPES-buffered saline (HBS, in mM, NaCl 130, KCl 3.5, $CaCl_2$ 2, $MgCl_2$ 1.2, HEPES 10 pH 7.4, glucose 10). Cells were voltage clamped using single patch electrodes in the whole-cell mode and held at −65 mV using an Axon Instruments model 200A amplifier. Patch pipets were made from 1.65 mm o.d. 7052 glass (Garner Glass) and pulled to a resistance of 2−5 MΩ using a Sutter Instruments P87 puller. The voltage clamp electrode solution contained 140 mM KCl, 2 mM $MgCl_2$, 2 mM 1,2-bis (2-aminophenoxy)ethane- *N*,*N*,*N*′,*N*′-tetraacetic acid (BAPTA), 2 mM $CaCl_2$, 1 mM HEPES, pH 7.4. Voltage clamp protocols were controlled using the pCLAMP (v. 6.2, Axon Instruments) suite of programs. In the current−clamp configuration the holding potential was removed and intracellular voltage was measured relative to the bath. The NG108 cells on the supporting NP films demonstrate features of differentiation into healthy cells expressing neuronal phenotype, showing smooth membranes, extension of complex neurites (Figure 2), and typical voltage-activated inward currents under whole-cell stimulation (see Supporting Information, Figure S2).

When stimulated with a 532 nm laser (Figure 3AB) (fluence ca. 800 mW/cm^2), cells grown on (PDDA/HgTe)$_{12}$PLP showed electrophysiological responses indicative of photostimulated activation. Under voltage-clamp, NG108 cells held at −65 mV showed an instantaneous inward current (Figure 3A) that corresponded with the time-

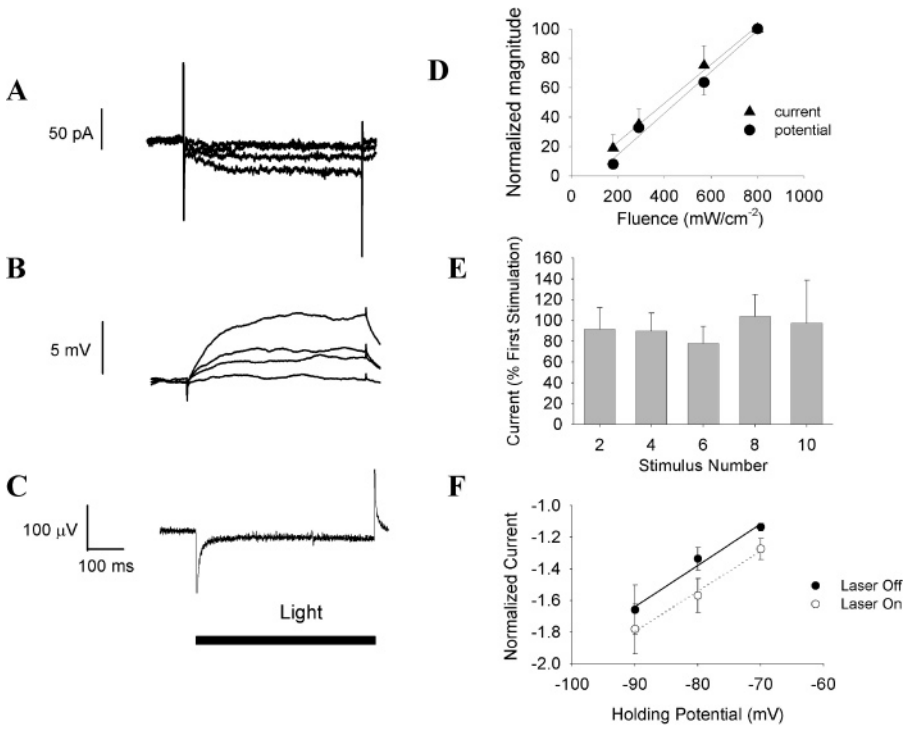

Figure 3. Light-induced electrophysiological effects in NG108 cells attached to $(PDDA/HgTe)_{12}PLP$ films. (A). Representative current traces of different cells held at −65 mV in voltage-clamp mode at different light fluences. Cells were photostimulated with a frequency-doubled diode laser at 532 nm for 500 ms at 0.1 Hz in constant wavelength mode. Illumination was at 45° to the NP film surface, and the spot size was approximately 1−1.5 mm in diameter. (B**)** Membrane potential changes measured in current-clamp mode. **(**C**)**. Light-induced potential change in the NP film measured with a micropipet recorded by placing the patch electrode in the bath adjacent to but outside of the cell. **(**D**)** Photoresponse of cells at different light fluencies averaged for three different cells. Each point is an average of five traces; the data were normalized to the current or potential change recorded at 800 mW/cm^2. Each cell was tested at all fluencies. Here and elsewhere error bars are standard error of the mean repetitive response of three cells. Trend lines were predicted by the least-squares linear regression **(**E**)**. Dependence of photoinduced cell current on pulse number normalized to the current in first pulse. The data were averaged for 15, 15, 12, 11, and 8 cells for the second, fourth, sixth, eighth, and tenth pulse, respectively. Additionally, currents from cells where the strong antioxidant ascorbic acid (5 mM) was added were equal in magnitude to of those recorded without antioxidant, indicating that the cells were not stimulated by a light-induced oxidation of membrane components. The efficient scavenging of oxygen radicals by ascorbates (vitamin C) is well-known. (F) Leak currents averaged for three different cells, measured by generating 100 ms voltage steps from −65 mV to −90, −80, and −70 mV. The magnitude of the current responses was determined as the mean current value between 90 and 100 ms. Data were normalized on the dark current at −65 mV. Each cell was tested at all potentials. Error bar is the standard error of the mean normalized current. Trend lines were predicted by the least-squares linear regression.

course of the stimulation of the thin film (Figure 3C). Similarly, the photostimulus resulted in depolarization of the cell (Figure 3B), which could be recorded in current clamp mode. The membrane potential traces on $(PDDA/HgTe)_{12}PLP$ showed plateaus after 100−200 ms. Cells recorded on $(PDDA/HgTe)_{12}$ PLP showed a mean depolarization magnitude of 2.3 ± 2.4 mV (range = 0−8.6 mV, 28 cells), but this included cells that showed no coupling to the surface at all (<0.5 mV depolarization $n = 8$). However, individual photostimulated depolarizations over 10 mV were observed, and these did lead to the generation of regenerative voltage changes characteristic of APs (Figure 4A,C) in one of 28 cells. This indicated to us that nanostructured devices from quantum-confined NPs were capable of exciting the cells but that a more efficient and biocompatible interface between the NP film and the cell could result in more reliable coupling of the photoactivation and cell stimulation.

Further studies of cells grown on $(PDDA/HgTe)_{12}PLP$ confirmed coupling of cell stimulation to photoelectric current generation. A linear relationship between the light fluence and the magnitude of current or voltage response (Figure 3D, Figure 3A,B) is associated with single-photon (i.e., linear) charge carrier generation in NP multilayer films in $(PDDA/HgTe)_{12}PLP$ (Supporting Information Figure S1). These findings were consistent with the proposed mechanism based on $NP \rightarrow O_2$ charge transfer (Figure 1A). No oxidative damage or additional cell stimulation was observed for a repetitive train of pulses (Figure 3E), as membrane resistance did not change throughout a train of stimuli. Additionally, cells cultured on glass with the same optical density as the NP films did not show response to illumination, suggesting that a thermal mechanism or direct light gating of neurons was not responsible for photoinduced stimulation in this system.[37,38] The absence of thermal excitation can also be confirmed by simple thermodynamic calculations presented in Supporting Information. No oxidative damage or additional cell stimulation was observed for a repetitive train of pulses (Figure 3E), as membrane resistance did not change throughout a train of stimuli. All these findings are consistent with the proposed mechanism based on $NP \rightarrow O_2$ charge transfer (Figure 1A).

The current−voltage relationships were examined to understand better the mechanism of the photoactivation. If

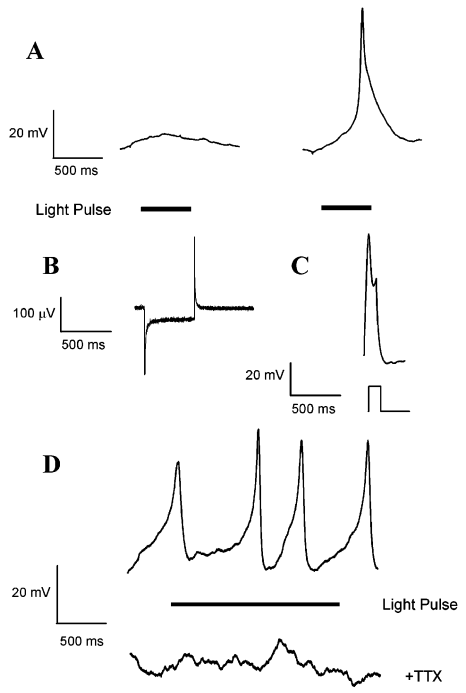

Figure 4. Light-induced action potentials in NG108 cells grown on LBL HgTe films. (A) Subthreshold membrane potential changes (left trace) and AP (right trace) recorded in one NG108 cell. (B) Photopotential recorded from the nanoparticle thin film using a microelectrode placed just over the film surface. (C) Regenerative potential change, obtained by injection of a 0.5 nA, 100 ms current pulse into the cell. Note that this potential change shows similar time course and magnitude to that demonstrated by photoactivation. (D) NG108 cells grown on $(PDDA/HgTe)_{12}$ + $(PDDA/Clay)_2$ showing multiple action potential spikes when given a long (2 s) photostimulus (upper trace). Cells did not demonstrate action potential response when treated with 100 nM TTX (lower trace).

light quanta directly opened or closed ion channels, there would be a membrane conductance change revealed in the current−voltage curve. Measurement of the cell response to hyperpolarizing voltage steps revealed parallel current−voltage relationships in control and light-stimulated NG108 cells (Figure 3F). This strongly suggested that no new ion conductive pathways were activated or inhibited as a result of photostimulation,[39] and indicated that the photocurrent generated in the $(PDDA/HgTe)_{12}PLP$ acted as an extrinsic current source that flows across the membrane rather than an intrinsic response that directly gates ion channels.[40]

In addition to improved biocompatibility, the LBL method also offers the possibility to engineer an increase in the neural response to light. This is critically important for future development of the technology of neuronal interfaces and fine-tuning of neural response in nanobio devices. LBL films of clay sheets, which represent nanoscale version of nacre,[41] possess high dielectric constant (ca. $\epsilon = 130-325$) and excellent ionic conductivity.[42,43] Both of these factors can help generate sufficient potential difference at the clay−membrane interface and ionic currents through the membrane. The possibility of balancing of electronic and ionic currents in the vicinity of the cell membranes is one of the key advantages of the NP LBL films compared to a metal or silicon interface. Additionally, clay minerals are known to adsorb oxygen,[44] which can also be used in NP→O_2 photoreaction. Finally, clay is an alumosilicate, and therefore, chemically similar to silicon oxide, which is known to be biocompatible with neurons.[25]

PDDA/montmorillonite clay bilayers, $(PDDA/Clay)_N$, were deposited on top of $(PDDA/HgTe)_{12}$. The cathodic capacitive spike at the light "turn-on" point increased from 4 μA to 11.5 μA and 7.5 μA for $N = 0$, 1, and 2, respectively (Supporting Information, Figure S4). For additional LBL layers, it is typical to reduce the rate of electrochemical reactions which can be seen both for clay, nanoparticle,[29] and graphite oxide LBL films;[45] however, it is quite unusual to increase it as for $N = 1$. The photocurrent decreased upon further addition of (PDDA/Clay) layers due to the slow diffusion of oxygen in clay layers.[46] NG108 cells grown on $(PDDA/HgTe)_{12}(PDDA/Clay)_2PLP$ showed mean photostimulated currents of 2.7 ± 3.4 pA (9 cells) with a higher mean magnitude of depolarization (4.8 ± 5.4 mV). The increase in depolarization magnitude with lower currents is probably the result of an increase in membrane resistance in cells cultured on $(PDDA/HgTe)_{12}(PDDA/Clay)_2PLP$ (136 ± 21 MΩ, $n = 21$, versus 119 ± 70 MΩ $n = 8$ without clay) and is indicative of better cell integrity on the more biocompatible clay nanolayers. More importantly, in cells that showed coupling of photoactivation to AP production, depolarization prior to AP was 10 mV.

Despite some cell heterogeneity, we observed generation of APs in a greater subpopulation of cells grown on $(PDDA/HgTe)_{12}(PDDA/Clay)_2PLP$ (11% or 7 of 63, Figure 4A,C,D) than without the clay layers. Because only 70% (27 of 37) of the cells given a current injection of 0.5−2 nA showed APs, these numbers underestimate the percentage of cells that respond to light. Photoactivated APs in NG108 could be blocked by inhibiting voltage-gated Na^+ channels (Figure 4D). Repetitive APs of an NG108 cell grown on $(PDDA/HgTe)_{12}(PDDA/Clay)_2PLP$ were suppressed by 100 nM of tetrodotoxin (TTX), which confirms physiological similarity of photoinduced APs to those typically observed in NG108-15.

Several mechanisms for photoinduced stimulation of neurons have been proposed and tested, and each has a unique set of challenges for applications in biomedicine and bioengineering. Perhaps the most promising of these involve heterologous expression of genetically engineering ion channels to convey light sensitivity to neurons.[40,47−50] These methods rely on the delivery of genetically engineered materials to specific cells. Biomedical applications of these technologies will necessitate a more precise gene targeting and gene expression control before they are feasible. Bulk silicon semiconductor materials have been used in more traditional photocurrent generation schemes to delivery spatially restricted stimulation to neurons in vitro[51,52] and photodiodes are currently being tested as retinal prostheses.[53] Photocurrent generation in these bulk materials is robust and distinct from our proposed mechanism for nanostructured films. The "top-down" fabrication of biomedical devices from these materials is currently ongoing, but there will be significant challenges in the materials flexibility, configu-

ration, and transparency for the small, irregular and delicate surfaces of neural and neuroepithelial tissues. Studies have also utilized direct stimulation of nerves and cells with light.[38,54,55] To date, the mechanism of this direct photostimulation is unclear and needs to be resolved to rule out an oxidative changes to the membrane[55] or thermal and photonic damage to cells.

Our system is unique in that it utilizes a nanostructured surface mechanism of photocurrent generation. Fabrication of the thin film is "bottom-up," and LBL can be adapted to engineer a great variety of patterns, electrical responses, optical properties, and material properties. Although semiconductor NPs have demonstrated some toxicity, methods to enhance their biocompatibility are rapidly evolving.[56] Biocompatibility and generation of efficient photoelectric materials will be a continuing subject of discussion to nanostructured thin films, and there are means to improve it especially when the structure of the LBL films can be controlled so easily.[34]

Our results also indicated a method of coupling light to the neuronal response that was distinct from those in the studies listed above. Our neurons showed a resistive coupling of the photocurrent to cell stimulation, in contrast to a direct change in membrane conductance with light-activated ion channels or capacitive coupling for bulk semiconductor devices.[52] The photoelectric current generation is characterized by a rapid charge buildup on the interface (the negative spike in Figures 1A, 1C, and 3C), which is quickly resolved by electrons donated from the ITO support. However, except for a small negative capacitive spike (Figure 3B) due to the negative ion buildup on the cell side of the membrane, there is no sustained physiological response from neurons to this stimulation. Capacitive stimulation of neurons, as observed by Fromherz and colleagues,[25] would result in rapid AP generation on the decaying phase of the fast voltage spike, but cell response is not seen until much later (Figure 3B vs Figure 3C or Figure 4A,B vs Figure 4C). This argues against the stimulation via capacitive coupling mechanisms as proposed for a neuron/silicon interface

Cell depolarization was seen during the direct current (dc) phase of the photostimulation. The resulting cell stimulation (AP generation) can be described as "resistive coupling": photogenerated current flowing across the resistance of the membrane results a relative depolarization of the cell, leading to AP generation. This mechanism is supported by several experimental facts. (1) The current−voltage relationship for hyperpolarizing holding potentials under illumination was parallel to that in the dark (Figure 3F), which indicated that resistance, *R*, is the same with or without light. This is in contrast to a mechanism that opens or closes channels or membranes as a result of illumination.[40,55] (2) The cell response upon illumination intensity was linear because for weak stimuli *R* remains constant regardless of the ionic flow. (3) The time course of the photoinduced membrane potential (parts A and B of Figure 3), was approximately equal to the RC time constant (75 ms, three cells) measured by current injection into NG108. This is characteristic of an extrinsically induced response. Thus, the resistive mechanism can successfully explain both the temporal profile of voltage transients (Figure 3A,B) and parallel current−voltage characteristics (Figure 3F); it is also consistent with the dynamics of photoelectric current generation in the nanobiodevice. In this respect, the LBL layers of montmorillonite and other clays are likely to provide additional benefits beyond the increase of the intrinsic photopotential and improvement of biocompatibility. Ion transport in clay multilayers occurs through stochastically formed ion channels, which may concentrate the current in specific areas. If the cell happen to be located on top of the ion-channel in the multilayer, it will be stimulated substantially stronger than the other, which explains along with other factors the fact that only a subpopulation of the adhered cells displayed AP.

To summarize the findings of this study, we have demonstrated (1) stimulation of a model neuron cell by photocurrent generated from light quanta absorbed in quantum-confined NP thin films. These currents were capable of generating APs in the neuronal cells, and therefore, the light excitation event can be communicated to the outside system or to other neurons. (2) Nanoscale engineering of the interface between the neuronal cell and NP film by the LBL technique could enhance the coupling of electrical and ion transport properties, which may be further adapted for different neural nanobiodevices. Our hypothesized resistive coupling mechanism can potentially be a robust substitute for capacitive coupling because it is may be less sensitive to gap fluctuations and accumulation of biological materials at the electrode−cell interface.

In perspective, utilization of nanomaterials provides new opportunities for neuroprosthetic devices that can potentially include the development of brain−computer interface technologies with IR optical information input typical for modern information technologies. Assuming that some significant challenges, such as long-term biocompatibility and the maintenance of neuron−device contact can be solved, quantum effects in NPs can be used to tune the spectral sensitivity and electrical response in such devices. Development of method of nanoscale interface engineering is one of the key technologies necessary to address these challenges. We believe that nanocolloids will be an essential part of the engineering such interfaces.

Acknowledgment. N.A.K., M.M., and T.C.P. thank NSF for Biophotonics Initiative Grant #BES- 0119483. N.A.K. also thanks NSF CAREER for Grant #CHE-9876265 supporting this research. T.C.P. acknowledges NIDCD DC07105 for support. The authors acknowledge the help of B. N. Christensen (UTMB) and S. Prakhya with experiments done in the course of this work.

Supporting Information Available: AMF images of different neuron growth substrates with and without NP coatings, dependence of the peak cathodic photocurrent on the intensity of the incident light, cell current recorded in whole cell voltage clamp of NG108, and evaluation of thermal excitation of neurons. This material is available free of charge via the Internet at http://pubs.acs.org.

References

(1) Bruchez, M., Jr.; Moronne, M.; Gin, P.; Weiss, S.; Alivisatos, A. P. *Science* **1998**, *281*, 2013−2016.
(2) Mirkin, C. A.; Letsinger, R. L.; Mucic, R. C.; Storhoff, J. J. *Nature* **1996**, *382*, 607−609.
(3) Cui, Y.; Wei, Q.; Park, H.; Lieber, C. M. *Science* **2001**, *293*, 1289.
(4) Han, J.; Craighead, H. G. *Science* **2000**, *288*, 1026.
(5) Hirsh, R.; Stafford, R. J.; Bankson, J. A.; Sershen, S. R.; Rivera, B.; Price, R. E.; Hazle, J. D.; Halas, N. J.; West, J. L. *Proc. Natl. Acad. Sci. U.S.A.* **2003**, *100*, 13549−13554.
(6) Zhang, Z.; Yang, X.; Zhang, Y.; Zeng, B.; Wang, S.; Zhu, T.; Roden, R. B. S.; Chen, Y.; Yang, R. *Clin. Cancer Res.* **2006**, *12* (16), 4933−4939.
(7) Kam, N. W. S.; O'Connell, M.; Wisdom, J. A.; Dai, H. *Proc. Natl. Acad. Sci. U.S.A.* **2005**, *102* (33), 11600−11605.
(8) Lu, Q.; Moore, J. M.; Huang, G.; Mount, A. S.; Rao, A. M.; Larcom, L. L.; Ke, P. C. *Nano Lett.* **2004**, *4* (12), 2473−2477.
(9) Cuenca, A. G.; Jiang, H.; Hochwald, S. N.; Delano, M.; Cance, W. G.; Grobmyer, S. R. *Cancer* **2006**, *107* (3), 459−466.
(10) Liao, H.; Nehl, C. L.; Hafner, J. H. *Nanomedicine* **2006**, *1* (2), 201−208.
(11) Zhang, J.; Lan, C. Q.; Post, M.; Simard, B.; Deslandes, Y.; Hsieh, T. H. *Cancer Genomics Proteomics* **2006**, *3 (*3−4), 147−158.
(12) Peppas, N. A.; Hilt, J. Z.; Khademhosseini, A.; Langer, R. *Adv. Mater.* **2006**, *18* (11), 1345−1360.
(13) Vonarbourg, A.; Passirani, C.; Saulnier, P.; Benoit, J. P. *Biomaterials* **2006**, *27* (24), 4356−4373.
(14) Xu, Z. P.; Zeng, Q. H.; Lu, G. Q.; Yu, A. B. *Chem. Eng. Sci.* **2005**, *61* (3), 1027−1040.
(15) LaVan, D. A.; McGuire, T.; Langer, R. *Nat. Biotechnol.* **2003**, *21*, 1184.
(16) Turner, J. N. *Exp. Neurol.* **1999**, *156*, 33.
(17) Ben Nissan, B.; Milev, A.; Vago, R. *Biomaterials* **2004**, *25*, 4971.
(18) Gheith, M. K.; Pappas, T.; Motamedi, M.; Kotov, N. A. *Adv. Mater.* **2006**, *18*, 2975−2979.
(19) Wang, K.; Fishman, H. A.; Dai, H.; Harris, J. S. *Nano Lett.* **2006** *6* (9), 2043−2048.
(20) Gheith, M. K.; Sinani, V. A.; Wicksted, J. P.; Matts, R. L.; Kotov, N. A. *Adv. Mater.* **2005** *17* (22), 2663−2670.
(21) Lovat, V.; Pantarotto, D.; Lagostena, L.; Cacciari, B.; Grandolfo, M.; Righi, M.; Spalluto, G.; Prato, M.; Ballerini, L. *Nano Lett.* **2005** *5* (6), 1107−1110.
(22) Hu, H.; Ni, Y.; Mandal, S. K.; Montana, V.; Zhao, B.; Haddon, R. C.; Parpura, V. *J. Phys. Chem. B* **2005** *109* (10), 4285−4289.
(23) McKenzie, J. L.; Waid, M. C.; Shi, R.; Webster, T. J. *Biomaterials* **2004** *25* (7−8), 1309−1317.
(24) Patolsky, F.; Timko, B. P.; Yu, G.; Fang, Y.; Greytak, A. B.; Zheng, G.; Lieber, C. M. *Science* **2006**, *313* (5790), 1100−1104.
(25) Fromherz, P. *Chem. Phys Chem.* **2002**, *3* (3), 276−284.
(26) Decher, G. *Science* **1997**, *277* [5330], 1232−1237.
(27) Mamedov, A. A.; Belov, A.; Giersig, M.; Mamedova, N. N.; Kotov, N. A. *J. Am. Chem. Soc.* **2001**, *123* (31), 7738−7739.
(28) Mamedov, A.; Ostrander, J.; Aliev, F.; Kotov, N. A. *Langmuir* **2000**, *16* (8), 3941−3949.
(29) Kotov, N. A.; Dekany, I.; Fendler, J. H. *J. Phys. Chem.* **1995**, *99* (35), 13065−13069.
(30) Rogach, A. L.; Koktysh, D. S.; Harrison, M.; Kotov, N. A. *Chem. Mater.* **2000**, *12* (6), 1526−1528.
(31) Cassagneau, T.; Mallouk, T. E.; Fendler, J. H. *J. Am. Chem. Soc.* **1998** *120* (31), 7848−7859.
(32) Hamprecht, B.; Glaser, T.; Reiser, G.; Bayer, E.; Propst, F. *Methods Enzymol.* **1985**, *109*, 316−341.
(33) Brown, D. A.; Higashida, H. *Physiology* **1988**, *397*, 165.
(34) Sinani, V. A.; Koktysh, D. S.; Yun, B. G.; Matts, R. L.; Pappas, T. C.; Motamedi, M.; Thomas, S. N.; Kotov, N. A. *Nano Lett.* **2003**, *3* (9), 1177−1182.
(35) Picart, C.; et al. *Mater. Res. Soc. Symp. Proc.* **2004**, *823*, 225.
(36) Pierschbacher, M. D.; Ruoslahti, E. *Nature* **1984**, *309*, 30−33.
(37) Hirase, H.; Nikolenko, V.; Goldberg, J. H.; Yuste, R. *J. Neurobiol.* **2002**, *51* (3), 237−247.
(38) Wells, J.; Kao, C.; Mariappan, K.; Albea, J.; Jansen, E. D.; Konrad, P.; Mahadevan-Jansen, A. *Opt. Lett.* **2005**, *30* (5), 504−506.
(39) Furakawa, T.; Furshpan, E. *J. Neurophysiol.* **1963**, *26*, 140−176.
(40) Banghart, M.; Borges, K.; Isacoff, E.; Trauner, D.; Kramer, R. H. *Nat. Neurosci.* **2004**, *7* (12), 1381−1386.
(41) Tang, Z.; Kotov, N. A.; Magonov, S.; Ozturk, B. *Nat. Mater.* **2003**, *2* (6), 413−418.
(42) Durstock, M.; Rubner, M. *Langmuir* **2001**, *17* (25), 7865−7872.
(43) Tedeschi, C.; Moehwald, H.; Kirstein, S. *J. Am. Chem. Soc.* **2001**, *123* (5), 954−960.
(44) Zhu, H. Y.; Vansant, E. F.; Lu, G. Q. *J. Colloid Interface Sci.* **1999**, *210* (2), 352−359.
(45) Kotov, N. A.; Dékány, I.; Fendler, J. H. *Adv. Mater.* **1996**, *8*, 637−641.
(46) Kotov, N. A.; Magonov, S.; Tropsha, E. *Chem. Mater.* **1998**, *10* (3), 886−895.
(47) Bayley, H. *Nat. Chem. Biol.* **2006**, *2* (1), 11−13.
(48) Boyden, E. S.; Zhang, F.; Bamberg, E.; Nagel, G.; Deisseroth, K. *Nat. Neurosci.* **2005**, *8* (9), 1263−1268.
(49) Lima, S. Q.; Miesenboeck, G. *Cell* **2005**, *121* (1), 141−152.
(50) Zemelman, B. V.; Lee, G. A.; Ng, M.; Miesenbock, G. *Neuron* **2002**, *33* (1), 15−22.
(51) Colicos, M. A.; Collins, B. E.; Sailor, M. J.; Goda, Y. *Cell.* **2001**, *107* (5), 605−616.
(52) Starovoytov, A.; Choi, J.; Seung, H. S. *J. Neurophysiol.* **2005**, *93* (2), 1090−1098.
(53) Chow, A. Y.; Chow, V. Y. *Neurosci. Lett.* **1997**, *225* (1), 13−16.
(54) Callaway, E. M.; Yuste, R. *Curr. Opin. Neurobiol.* **2002**, *12* (5), 587−592.
(55) Hirase, H.; Nikolenko, V.; Goldberg, J. H.; Yuste, R. *J. Neurobiol.* **2002**, 237−247.
(56) Derfus, A. M.; Chan, W. C. W.; Bhatia, S. N. *Nano Lett.* **2004**, *4* (1), 11−18.

NL062513V